

Cite this: *Chem. Sci.*, 2023, **14**, 14146

All publication charges for this article have been paid for by the Royal Society of Chemistry

## Understanding divergent substrate stereoselectivity in the isothiourea-catalysed conjugate addition of cyclic $\alpha$ -substituted $\beta$ -ketoesters to $\alpha,\beta$ -unsaturated aryl esters<sup>†</sup>

Ding Yuan,<sup>ab</sup> Alister S. Goodfellow,<sup>b</sup> Kevin Kasten,<sup>a</sup> Zhuan Duan,<sup>b</sup> Tengfei Kang,<sup>b</sup> David B. Cordes,<sup>b</sup> Aidan P. McKay,<sup>a</sup> Michael Bühl,<sup>b</sup> Gregory R. Boyce<sup>b</sup> <sup>\*acd</sup> and Andrew D. Smith<sup>b</sup> <sup>\*a</sup>

The development of enantioselective synthetic methods capable of generating vicinal stereogenic centres, where one is tetrasubstituted (such as either an all-carbon quaternary centre or where one or more substituents are heteroatoms), is a recognised synthetic challenge. Herein, the enantioselective conjugate addition of a range of carbo- and heterocyclic  $\alpha$ -substituted  $\beta$ -ketoesters to  $\alpha,\beta$ -unsaturated aryl esters using the isothiourea HyperBTM as a Lewis base catalyst is demonstrated. Notably, divergent diastereoselectivity is observed through the use of either cyclopentanone-derived or indanone-derived substituted  $\beta$ -ketoesters with both generating the desired stereodefined products with high selectivity (>95:5 dr, up to 99:1 er). The scope and limitations of these processes are demonstrated, alongside application on gram scale. The origin of the divergent substrate selectivity has been probed through the use of DFT-analysis, with preferential orientation driven by dual stabilising CH···O interactions. The importance of solvation with strongly polar transition-states is highlighted and the SMD solvation model is demonstrated to capture solvation effects reliably.

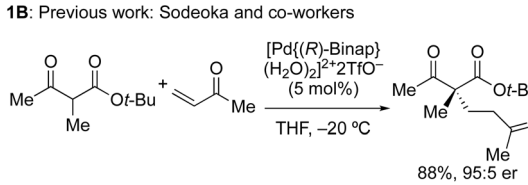
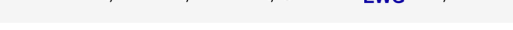
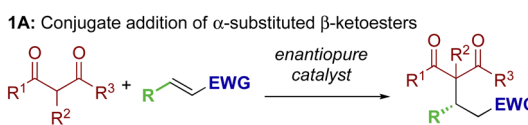
Received 15th October 2023  
Accepted 20th November 2023

DOI: 10.1039/d3sc05470e  
[rsc.li/chemical-science](http://rsc.li/chemical-science)

## 1 Introduction

The ability to selectively control the relative and absolute configuration in compounds containing vicinal stereogenic centres, where one is tetrasubstituted (defined herein as a stereogenic carbon that does not have a proton as a substituent) is of significant interest. Despite many advances in the development of synthetic methods in this area,<sup>1,2</sup> this still remains a meaningful challenge due to the generally low reactivity of suitable precursors caused by steric encumbrance. Among methods developed in this area, the enantioselective conjugate addition of  $\alpha$ -substituted  $\beta$ -ketoesters has been widely explored based on the ability to generate up to two contiguous

stereocentres, one of them quaternary (Scheme 1A).<sup>3,4</sup> As representative examples, this strategy has been applied to the stereoselective addition to nitro-olefins,<sup>5–7</sup> di-*t*-butyl azodicarboxylate,<sup>8,9</sup> vinyl ketones,<sup>10</sup> and propargyl alcohols.<sup>11</sup> For example, Sodeoka *et al.* showed that enantioselective addition of various  $\alpha$ -substituted  $\beta$ -ketoesters to enones proceeded in good yields with excellent enantioselectivity using Pd-BINAP derived enolates (Scheme 1B).<sup>12</sup> Alternatively, the Pd-catalysed



Scheme 1 Context: enantioselective conjugate addition of  $\alpha$ -substituted  $\beta$ -ketoesters.

<sup>a</sup>EaStCHEM, School of Chemistry, University of St Andrews, St Andrews, Fife, KY16 9ST, UK. E-mail: [ads10@st-andrews.ac.uk](mailto:ads10@st-andrews.ac.uk); [buehl@st-andrews.ac.uk](mailto:buehl@st-andrews.ac.uk)

<sup>b</sup>School of Biological and Chemical Engineering, Panzhihua University, Panzhihua 617000, China

<sup>c</sup>Department of Chemistry and Physics, Florida Gulf Coast University, Fort Myers, Florida 33965, USA

<sup>d</sup>Department of Chemistry and Biochemistry, East Stroudsburg University, East Stroudsburg, Pennsylvania 18301, USA. E-mail: [gboyce@esu.edu](mailto:gboyce@esu.edu)

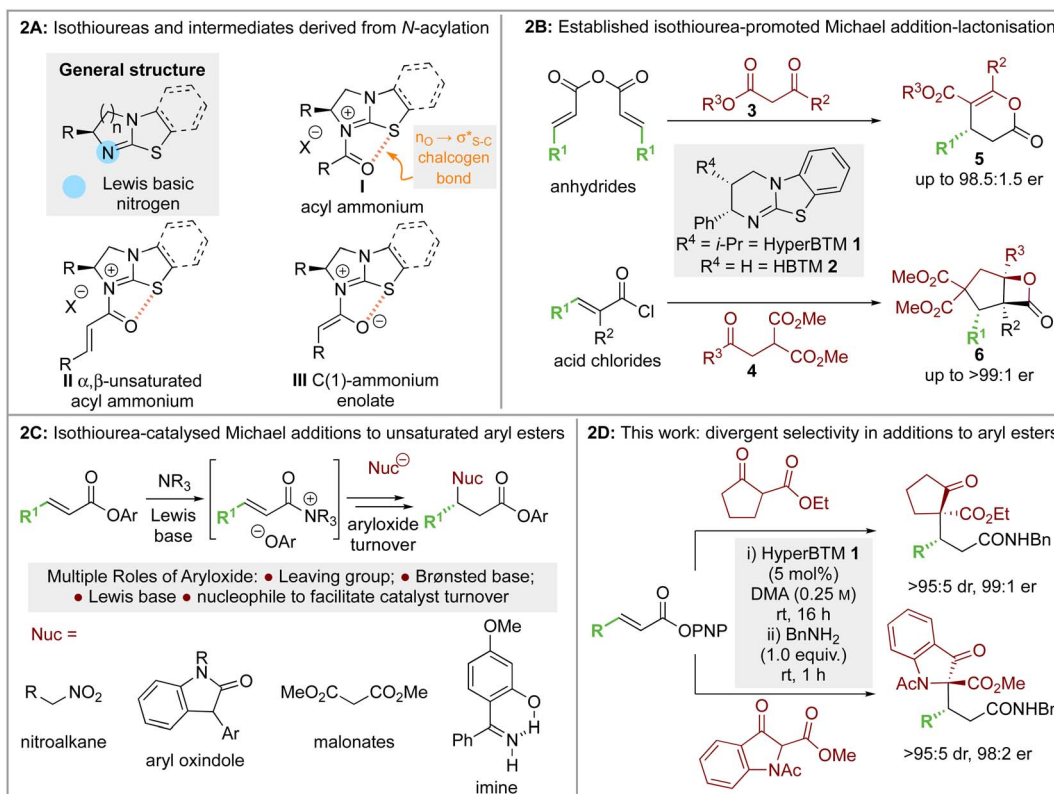
<sup>†</sup> Electronic supplementary information (ESI) available: Full characterisation, HPLC spectra and computational data. CCDC 2298980–2298982. For ESI and crystallographic data in CIF or other electronic format see DOI: <https://doi.org/10.1039/d3sc05470e>

allylic alkylation of Morita–Baylis–Hillman adducts has also been developed with  $\beta$ -ketocarbonyls.<sup>13</sup> Despite these precedents, stereoselective conjugate additions of  $\alpha$ -substituted  $\beta$ -ketoesters to  $\alpha,\beta$ -unsaturated esters is rare due to the low inherent electrophilicity of these Michael acceptors.

The use of isothioureas as Lewis basic organocatalysts has expanded remarkably over the last fifteen years. Building upon the pioneering work of Birman who demonstrated their first use as acyl transfer catalysts for kinetic resolution processes, these readily prepared chiral Lewis bases have since been harnessed for a plethora of transformations.<sup>14</sup> This broad range of reactivity incorporates the generation and reactivity of acyl ammonium I,<sup>14</sup>  $\alpha,\beta$ -unsaturated acyl ammonium II<sup>15</sup> and C(1)-ammonium enolate III<sup>16</sup> intermediates that exploit a key 1,5 S···O chalcogen bonding interaction ( $n_O$  to  $\sigma^*_S-C$ ) to achieve stereocontrol (Scheme 2A). Of relevance to this work, the generation and exploitation of  $\alpha,\beta$ -unsaturated acyl ammonium intermediates was initially achieved from acid chloride and anhydride starting materials. For example, isothioureas (2S,3R)-HyperBTM 1 and (S)-HBTM 2 have been employed in cascade processes with  $\beta$ -ketoesters 3<sup>17</sup> and  $\gamma$ -ketomalonates 4,<sup>18</sup> that involve initial Michael addition followed by *intramolecular* cyclisation to promote catalyst turnover, generating  $\delta$ - and  $\beta$ -lactones 5 and 6 (Scheme 2B). Related conjugate addition/cyclisation processes with acyl benzazoles,<sup>17,19</sup> amino-thiophenols,<sup>20</sup> heterocyclic nucleophiles,<sup>21</sup> as well as Rh-

metallacycles has been reported.<sup>22</sup> Joint synthetic and computational analysis of the factors leading to stereocontrol and chemoselectivity in acyl benzazole addition has led to enhanced understanding of these processes.<sup>23</sup>

In recent work, the use of  $\alpha,\beta$ -unsaturated electron-deficient aryl esters has been shown to offer a potential (albeit limited) solution to the recognised recalcitrance of  $\alpha,\beta$ -unsaturated esters to enantioselective conjugate addition (Scheme 2C). Acylation of these species with an isothiourea generates an  $\alpha,\beta$ -unsaturated acyl ammonium ion pair, with the enhanced electrophilicity of this intermediate species (compared to the parent ester) allowing for effective catalysis. Furthermore, the electron-deficient phenoxides generated *in situ* can be exploited to promote catalytic turnover, while their multifunctional nature can be exploited through acting as both Brønsted base and Lewis base.<sup>24</sup> Initially demonstrated in the enantioselective conjugate addition of nitroalkanes,<sup>19</sup> it has since been exploited using heterocyclic pronucleophiles,<sup>21,25</sup> malonates,<sup>26</sup> benzophenone imines,<sup>27</sup> as well as co-operative Pd-isothiourea promoted cascade reactions.<sup>28</sup> Conjugate addition and lactonisation processes using acylbenzothiazole and benzoxazole pronucleophile derivatives with  $\alpha,\beta$ -unsaturated *para*-nitrophenyl esters has also been investigated synthetically.<sup>29</sup> This study was complemented by a computational study by Wei and Ding who validated the postulated mechanism and outlined the key factors involved in stereoselective C–C bond-formation.<sup>30</sup>



**Scheme 2** (A) Isothioureas and common intermediates derived from *N*-acylation; (B) established isothiourea-promoted Michael addition-lactonisation; (C) isothiourea-catalysed addition to  $\alpha,\beta$ -unsaturated aryl esters; (D) this work: divergent substrate dependent selectivity in addition to  $\alpha,\beta$ -unsaturated aryl esters.



Building upon these previous studies, in this manuscript the enantioselective conjugate addition of a range of carbo- and heterocyclic  $\alpha$ -substituted  $\beta$ -ketoesters to  $\alpha,\beta$ -unsaturated aryl esters using the isothiourea HyperBTM 1 as a Lewis base catalyst is reported. Interestingly, divergent diastereoselectivity is observed with the use of either cyclopentanone-derived or indanone-derived substituted  $\beta$ -ketoesters, with both generating the desired stereodefined products with high selectivity ( $>95:5$  dr, up to  $99:1$  er, Scheme 2D). The origin of the divergent substrate selectivity has been probed using DFT-analysis at the M06-2X<sub>SMD</sub>/def2-TZVP//M06-2X<sub>SMD</sub>/def2-SVP level.

## 2 Results and discussion

### 2.1 Optimisation: conjugate addition of ethyl 2-oxocyclopentane-1-carboxylate to *p*-nitrophenyl 4,4,4-trifluorobut-2-enoate

Initial investigations began with developing the stereoselective reaction of ethyl 2-oxocyclopentane-1-carboxylate 7 (1.5 equiv.) with  $\beta$ -trifluoromethyl- $\alpha,\beta$ -unsaturated *p*-nitrophenyl (PNP) ester 8 using (2*S*,3*R*)-HyperBTM 1 (20 mol%) as the Lewis base catalyst. A benzylamine quench was performed after the catalytic transformation to aid product isolation. No reaction was observed in MeCN, CH<sub>2</sub>Cl<sub>2</sub> or EtOAc (entries 1–3). However, the use of amide solvents gave promising results, with NMP, DMF, and DMA giving between 40–70% conversion to the desired product (entries 4–6). Using DMA, further optimisation showed that reducing the equivalents of  $\beta$ -ketoester 7 and the catalyst loading to 5 mol% led to good reaction conversion (entries 7–

10), giving the desired product 9 in 57% isolated yield ( $>95:5$  dr,  $99:1$  er). Reaction conditions implementing a catalyst loading of 5 mol% was chosen as optimal to showcase the efficiency of this process at low catalyst loading (Table 1).

### 2.2 Scope and limitations

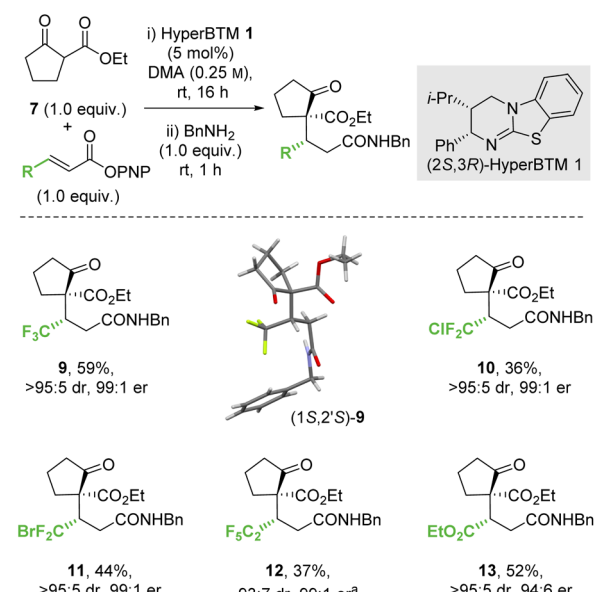
**2.2.1 Conjugate additions of ethyl 2-oxocyclopentane-1-carboxylate to  $\alpha,\beta$ -unsaturated *p*-nitrophenyl esters.** Further work considered the scope and limitations of this process initially through changing the  $\alpha,\beta$ -unsaturated *p*-nitrophenyl ester component of the reaction (Scheme 3). Under the developed conditions the incorporation of an electron withdrawing  $\beta$ -substituent was necessary to promote reactivity, with  $\beta$ -perhalogenated substrates giving the corresponding CF<sub>2</sub>Cl, CF<sub>2</sub>Br and C<sub>2</sub>F<sub>5</sub> variants 10–12 respectively in synthetically useful yield and excellent enantioselectivity ( $>95:5$  dr,  $99:1$  er). Similarly, a  $\beta$ -ester substituent was also tolerated, giving 13 in 52% yield,  $>95:5$  dr and  $94:6$  er. The relative and absolute configuration of (1*S*,2*S*)-9 was confirmed by single crystal X-ray crystallography,<sup>31</sup> with the configuration within all other products 10–13 assigned by analogy.

**2.2.2 Conjugate addition of  $\alpha$ -substituted carbo- and heterocyclic  $\beta$ -ketoesters to *p*-nitrophenyl 4,4,4-trifluorobut-2-enoate.** The effect of variation within the  $\alpha$ -substituted  $\beta$ -ketoester reaction component in the addition to  $\beta$ -trifluoromethyl- $\alpha,\beta$ -unsaturated PNP ester 8 (Scheme 4) was then examined. The incorporation of 3-oxopyrrolidine and 4-oxopyrrolidine scaffolds were successful, generating 14 and 15

Table 1 Initial optimisation<sup>a</sup>

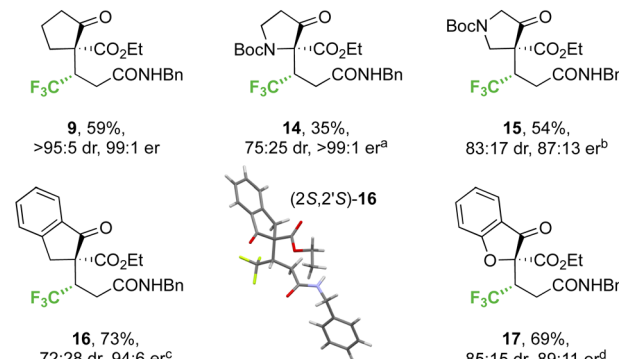
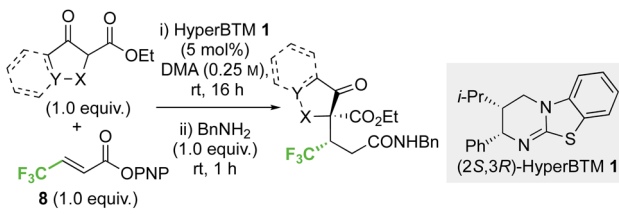
Entry	Solvent	HyperBTM 1 (mol%)	7 (equiv.)	Conversion <sup>b</sup>
1	MeCN	20	1.5	0
2	CH <sub>2</sub> Cl <sub>2</sub>	20	1.5	0
3	EtOAc	20	1.5	0
4	NMP	20	1.5	41
5	DMF	20	1.5	60
6	DMA	20	1.5	70
7	DMA	20	2.0	70
8	DMA	20	1.0	66
9	DMA	10	1.0	66
10	DMA	5	1.0	61 <sup>c</sup>

<sup>a</sup> Reactions performed on 0.5 mmol scale of 8. <sup>b</sup> Formation of product determined by <sup>19</sup>F NMR analysis of the crude reaction mixture by relative abundance of all fluorine signals in the sample. <sup>c</sup> Isolated in 57% yield,  $>95:5$  dr,  $99:1$  er; dr determined by <sup>1</sup>H NMR analysis of the crude reaction mixture, er determined by HPLC analysis on a chiral stationary phase. NMP = *N*-methylpyrrolidine, DMF = *N,N*-dimethylformamide, DMA = *N,N*-dimethylacetamide.



Scheme 3 Conjugate addition of ethyl 2-oxocyclopentane-1-carboxylate. All product yields were determined by HPLC analysis on a chiral stationary phase. All product drs were determined by <sup>1</sup>H NMR analysis of the crude reaction mixture. Following reaction conditions were applied unless stated otherwise: 0.2 mmol 7, 0.2 mmol *p*-nitrophenol ester, 0.01 mmol 1 were stirred in 0.8 mL DMA at rt for 16 h. Subsequently, 0.2 mmol BnNH<sub>2</sub> was added and stirred at rt for 1 h. (a) Combined yield of inseparable diastereomers.

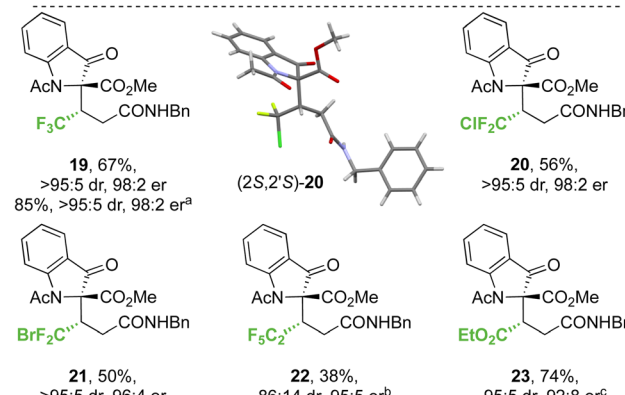
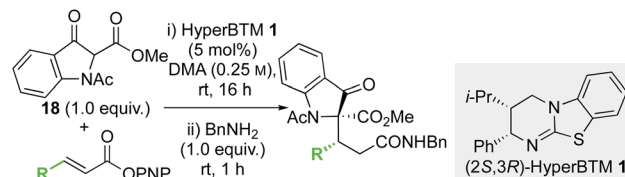




**Scheme 4** Conjugate addition of carbo- and heterocyclic  $\alpha$ -substituted  $\beta$ -ketoesters to  $\alpha,\beta$ -unsaturated *p*-nitrophenyl esters. All product drs were determined by HPLC analysis on a chiral stationary phase. All product drs were determined by  $^1\text{H}$  NMR analysis of the crude reaction mixture. Following reaction conditions were applied unless stated otherwise: 0.2 mmol ketoester, 0.2 mmol **8**, 0.01 mmol **1** were stirred in 0.8 mL DMA at rt for 16 h. Subsequently, 0.2 mmol  $\text{BnNH}_2$  was added and stirred at rt for 1 h. (a) 59 : 41 er of minor diastereomer, combined yield of inseparable diastereomers. (b) 97 : 3 er of minor diastereomer, combined yield of inseparable diastereomers. (c) 96 : 4 er of minor diastereomer, diastereomers isolated yields (major/minor): 51%/22%. (d) 95 : 5 er of minor diastereomer, combined yield of inseparable diastereomers.

respectively. Reduced yield (35%) and diastereoselectivity (75 : 25 dr) but high enantioselectivity (>99 : 1 er) was observed with the 3-oxopyrrolidine scaffold, whereas improved yield and high stereocontrol (54%, 83 : 17 dr, 87 : 13 er) were obtained in the 4-oxopyrrolidine case. The effect of benzannulation was next explored, with the dihydro-1*H*-indene derivative giving **16** (73%, 72 : 28 dr, 94 : 6 er). The relative and absolute configuration within the major diastereoisomer (*2S,2'S*)-**16** was confirmed by single crystal X-ray crystallography and correlates with that observed within product **9**,<sup>32</sup> with the configuration within all other products **14**, **15** and **17** assigned by analogy. The dihydrobenzofuran derivative was also successfully employed, giving heterocyclic product **17** (69%, 85 : 15 dr, 89 : 11 er).

**2.2.3 Conjugate additions of methyl 1-acetyl-3-oxoindolinone-2-carboxylate to  $\alpha,\beta$ -unsaturated *p*-nitrophenyl esters.** As both benzannulation and  $\alpha$ -heteroatom substitution within the  $\beta$ -ketoester reaction component had been tolerated their dual incorporation within an alternative scaffold, methyl 1-acetyl-3-oxoindolinone-2-carboxylate **18**, and its conjugate addition was assessed (Scheme 5). The conjugate addition of **18** to the  $\beta$ -trifluoromethyl- $\alpha,\beta$ -unsaturated PNP ester gave **19** in 67% yield (>95 : 5 dr, 98 : 2 er) on an analytical scale. A scaled-up synthesis on a 4.4 mmol scale allowed the formation of **19** in >1 g and 85% yield (>95 : 5 dr, 98 : 2 er) after direct

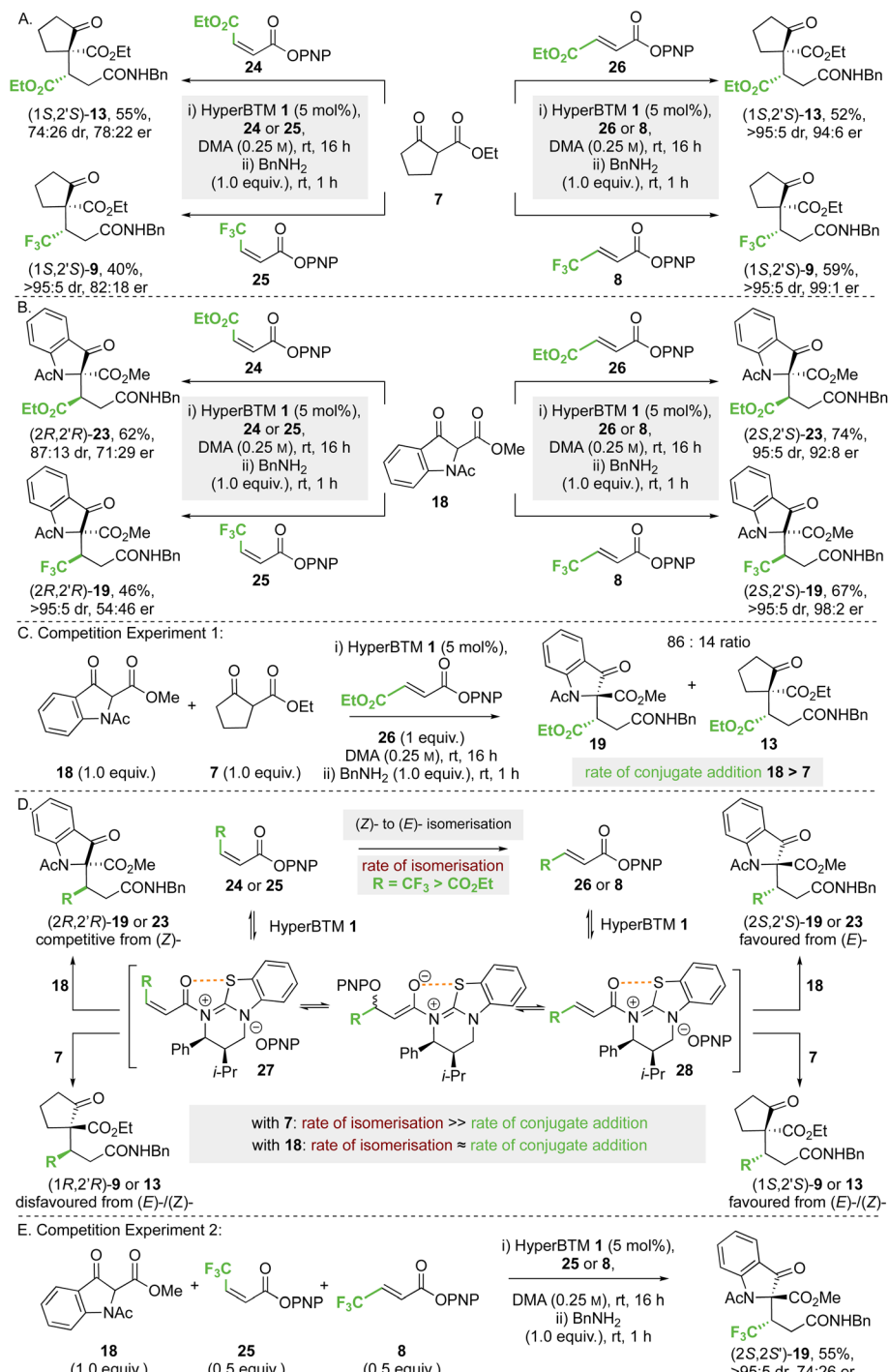


**Scheme 5** Conjugate addition of methyl 1-acetyl-3-oxoindolinone-2-carboxylate to  $\alpha,\beta$ -unsaturated *p*-nitrophenyl esters. All product drs were determined by HPLC analysis on a chiral stationary phase. All product drs determined by  $^1\text{H}$  NMR analysis of the crude reaction mixture. Following reaction conditions were applied unless stated otherwise: 0.2 mmol **18**, 0.2 mmol *p*-nitrophenol ester, 0.01 mmol **1** were stirred in 0.8 mL DMA at rt for 16 h. Subsequently, 0.2 mmol  $\text{BnNH}_2$  was added and stirred at rt for 1 h. (a) Reaction on a gram scale with purification by crystallisation. (b) 76 : 24 er of minor diastereomer, combined yield of inseparable diastereomers. (c) 72 : 18 er of minor diastereomer, combined yield of inseparable diastereomers.

recrystallisation from the crude reaction mixture. Application to alternative  $\beta$ -perhalogenated PNP esters gave the corresponding  $\text{CF}_2\text{Cl}$ ,  $\text{CF}_2\text{Br}$  and  $\text{C}_2\text{F}_5$  variants **20**–**22** respectively in acceptable yield (38% to 56%) and excellent stereoselectivity (>95 : 5 dr, 95 : 5 to 98 : 2 er). Further application of this methodology gave the  $\beta$ -ester variant **23** in 74% yield, 95 : 5 dr and 92 : 8 er. The relative and absolute configuration of (*2S,2'S*)-**20** was confirmed by single crystal X-ray crystallography,<sup>33</sup> with the configuration within all other products **19** and **21**–**23** derived from **18** assigned by analogy. Notably, in this system the relative configuration within the products is *opposite* to that previously observed at the stereogenic centre derived from the  $\beta$ -ketoester (section 2.2.1 and 2.2.2, note: CIP priority changes) consistent with divergent selectivity being observed for this reaction component.

**2.2.4 Conjugate additions to (*Z*)- $\beta$ -trifluoro- and (*Z*)- $\beta$ -ethoxycarbonyl  $\alpha,\beta$ -unsaturated *p*-nitrophenyl esters.** The effect of olefin configuration on product yield and stereoselectivity was next investigated using maleate **24** and fumarate **26**, as well as  $\text{CF}_3$ -substituted  $\alpha,\beta$ -unsaturated PNP ester derivatives (*Z*)-**25** and (*E*)-**8** (Scheme 6). Using ethyl 2-oxocyclopentane-1-carboxylate **7** as the nucleophile (Scheme 5A), reaction with maleate **24** gave product (*1S,2'S*)-**13** in the same enantiomeric series as fumarate **26**, but with reduced stereoselectivity (74 : 26 dr, 78 : 22 er). Using either  $\text{CF}_3$ -substituted (*Z*)-enoate **25** or (*E*)-enoate **8**, the same (*1S,2'S*)-stereoisomer of product **9** was





**Scheme 6** Effect of (*Z*)- or (*E*)-enoate configuration on stereoselectivity. All ers determined by HPLC analysis on a chiral stationary phase. All product drs determined by  $^1\text{H}$  NMR analysis of the crude reaction mixture. Yields are isolated yields after purification.

obtained in high dr and er (>95 : 5 dr, 82 : 18 er). Similar reactions were undertaken using methyl 1-acetyl-3-oxoindolinone-2-carboxylate **18** as the nucleophile (Scheme 6B); reaction with maleate **24** gave product (*2R,2'R*)-**23** in the *opposite enantiomeric series* to that derived from fumarate **26**, but with reduced stereoselectivity (87 : 13 dr, 71 : 29 er). Using  $\text{CF}_3$ -substituted (*Z*)-enoate **25**, the corresponding product **19** was obtained in high dr but in essentially *racemic* form (>95 : 5 dr, 54 : 46 er).

To decipher these results, competition experiment 1 (Scheme 6C) took a 50 : 50 ratio of nucleophiles **18** and **7** in the addition to fumarate **26**, giving an 86 : 14 ratio of products **19** and **13**. On the assumption of irreversible nucleophilic addition, this is consistent with the rate of addition of methyl 1-acetyl-3-oxoindolinone-2-carboxylate **18** being greater than that of ethyl 2-oxocyclopentane-1-carboxylate **7**. In addition, we considered previous work that showed both isothioureas and  $\text{NBu}_4\text{OPNP}$  can promote (*Z*)- to (*E*)-



enoate isomerisation,<sup>19,28a,34</sup> and that isomerisation of  $\text{CF}_3$ -substituted (*Z*)-enoates occurred at a significantly faster rate than that of maleates. Application to this case (Scheme 5D) would involve *N*-acylation of HyperBTM **1** with (*Z*)-**24** or (*Z*)-**25** to give the corresponding (*Z*)- $\alpha,\beta$ -unsaturated acyl ammonium ion pair **27**. Subsequent reversible conjugate addition of *para*-nitrophenolate (or HyperBTM **1**), followed by bond rotation and elimination, will lead to the thermodynamically favoured (*E*)-enoate *via* the corresponding (*E*)- $\alpha,\beta$ -unsaturated acyl ammonium ion pair **27** (Scheme 6D). Bringing this together, the observed experimental results in Scheme 6A and B can be understood based on the relative rates of nucleophilic addition of the  $\beta$ -ketoesters **18** and **7** to the (*E*)- or (*Z*)- $\alpha,\beta$ -unsaturated acyl ammonium intermediate **28** or **27**, alongside competitive (*Z*)- to (*E*)-enoate isomerisation. Using ethyl 2-oxocyclopentane-1-carboxylate **7** the rate of conjugate addition is slow relative to (*Z*)- to (*E*)-isomerisation, resulting in the same product enantiomer using either (*E*)- or (*Z*)-enoate as starting material. However, using methyl 1-acetyl-3-oxoindolinone-2-carboxylate **18**, the conjugate addition to an intermediate (*Z*)- $\alpha,\beta$ -unsaturated acyl ammonium species must occur at a faster rate than isomerisation of maleate **24**, giving preferentially the product antipode (*2R,2'R*)-**23** compared to the reaction with fumarate **26**. Using this argument, the effectively racemic nature of product **19** from  $\text{CF}_3$ -substituted (*Z*)-enoate **25** and **18** is assumed to arise from *approximately identical* rates of (*Z*)- to (*E*)-isomerisation and conjugate addition to the (*Z*)- $\alpha,\beta$ -unsaturated acyl ammonium species. To test this hypothesis, competition experiment 2 was designed and carried out (Scheme 6E). Using a 50 : 50 mixture of  $\text{CF}_3$ -substituted (*E*)-enoate **8** and (*Z*)-enoate **25** in the reaction of **18** was predicted to give an approximate 75 : 25 mixture of product (*2S,2'S*) : (*2R,2'R*)-enantiomers; in practice product **19** was isolated in 55% yield (>95 : 5 dr, 74 : 26 er), supporting this hypothesis.

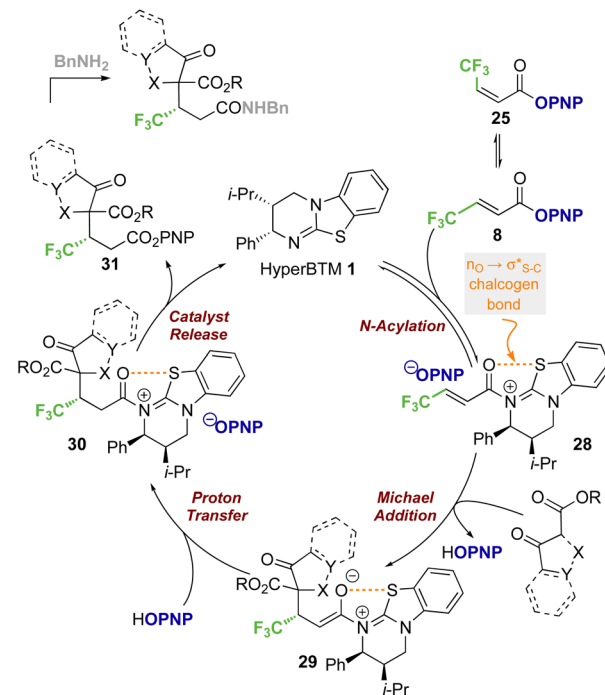
### 2.3 Proposed mechanism

Based on previous studies and the observations reported herein,<sup>19,26,28a,29,35</sup> a general and simplified catalytic cycle for this transformation can be proposed (Scheme 7). Isothiourea catalyst HyperBTM **1** undergoes reversible *N*-acylation with PNP ester **8**, generating  $\alpha,\beta$ -unsaturated acyl ammonium ion pair **28** with an  $\text{S}\cdots\text{O}$  conformational lock.<sup>23,36-43</sup> Deprotonation of the  $\beta$ -ketoester by the released *p*-nitrophenoxide, followed by subsequent stereoselective conjugate addition to the  $\alpha,\beta$ -unsaturated acyl isothiouronium intermediate **28** in the assumed stereodetermining step gives enolate **29**. Subsequent protonation, presumably by the generated *p*-nitrophenol, gives acyl-isothiouronium species **30**. The aryloxide subsequently effects catalyst turnover to afford *p*-nitrophenyl ester **31**, which upon treatment with benzylamine gives the corresponding amide product.

While this general mechanism accounts for the connectivity observed within the products, the divergent stereoselectivity observed with choice of pronucleophile was further investigated by DFT analysis.

### 2.4 DFT computation

To probe the origin of stereocontrol, DFT calculations at the M06-2X<sub>SMD</sub>/def2-TZVP//M06-2X<sub>SMD</sub>/def2-SVP level of theory



Scheme 7 Proposed simplified catalytic cycle.

were performed using Gaussian16.<sup>44-50</sup> Following the pioneering computational work by Cheong *et al.*<sup>23</sup> and Wang *et al.*<sup>30</sup> who identified the Michael addition (C–C bond formation) between a cationic HyperBTM-*N*-acyl complex and a C nucleophile (Scheme 6) as the stereodetermining step in isothiourea-catalysed conjugate addition cyclisation reactions, our computational modelling concentrated on that step. An extensive transition-state (TS) search was conducted, exploring the conformational freedom of the approaching nucleophile (see ESI†). The diastereoselectivity for the reaction was evaluated as the difference in free energy ( $\Delta\Delta^\ddagger G$ ) of the lowest TS leading to each of the diastereoisomeric products. From this extensive TS search, we found that the facial selectivity imposed by the catalyst was consistent with previous work, driven by the 1,5  $\text{S}\cdots\text{O}$  chalcogen interaction ( $n_\text{O}$  to  $\sigma^*_{\text{S-C}}$ ) between the acyl O and catalyst-derived S atom that provides a conformational lock, with reaction through the *s-cis* conformation.<sup>23,41</sup> This places the phenyl substituent perpendicular to the plane of the catalyst, with conjugate addition *anti*-to this unit to the *si*-face of the  $\alpha,\beta$ -unsaturated isothiouronium intermediate, consistent with the high enantioselectivity and absolute configuration observed.

Between the possible approaches towards the accessible *si*-face of the isothiouronium ion intermediate, substrate facial selectivity is driven by a variety of non-covalent interactions between the nucleophile and  $\alpha,\beta$ -unsaturated isothiouronium intermediate. For the addition of **7** to give preferentially **9**, dual non-classical  $\text{CH}\cdots\text{O}$  stabilising interactions between the acidic  $^+\text{NC-H}$  derived from the catalyst and the ketoester of the nucleophile are observed, accounting for the preferential orientation of the major and minor TS (86 : 41 dr, Fig. 1). Experimentally, benzannulation of **7** to give ethyl 1-oxo-2,3-



dihydro-1*H*-indene-2-carboxylate as the nucleophile leads to **16** with an observed reduction in dr (72 : 28 dr). This is qualitatively reproduced computationally (55 : 45 dr), with the major TS again stabilised by CH···O interactions between the benzylic <sup>+</sup>NC-H derived from the catalyst and nucleophile. In this case, the minor diastereoisomeric TS for **16** does not contain CH···O interactions, but instead exhibits a stabilising cation–π interaction due to the orientation of the benzannulated ring of the nucleophile with the isothiouronium ion within the acylated catalyst (Fig. 1a and b). This interaction slightly stabilises the minor TS, reducing the energy difference between the two diastereoisomeric TS and lowering the dr. This subtle interplay between cation–π and CH···O interactions is fully in line with findings by Wang *et al.* for a related Michael addition reaction.<sup>30</sup>

The divergent selectivity observed with indoline derived substrate **19** was also investigated. The computed major TS aligns with experiment, with the minor TS lacking in CH···O interactions. Instead, the minor TS features π-type interactions between the substrate acyl group and the isothiouronium acylated catalyst, analogous to the cation–π interaction of **16** (see Fig. 1b).

Importantly, the choice of implicit solvent model was found to dramatically impact the ability of the computational method to reproduce experimental results. These models allow for simple representation of the solvent as a continuous dielectric

but can become unreliable in the case of large dipole moments or charges. The chosen transition states are strongly zwitterionic composed of an anion derived from deprotonation of the β-ketoester and a cationic isothiouronium derived Michael acceptor.

Preliminary calculations using the Polarisable Continuum Model (PCM)<sup>51,52</sup> employed in previous studies<sup>26,50</sup> led to the incorrect prediction of the minor diastereoisomer of **16** (33 : 64 dr), arguably due to the poor treatment of solvation. Two alternate approaches identified the correct major diastereomer with PCM: explicit micro-solvation (85 : 15 dr, Fig. 1b) and increased scaling of the solvent cavity ( $\geq 1.15$  van der Waals radii, Fig. 1c). Micro-solvation adds an explicit solvent molecule to the DFT calculation, allowing for more accurate interaction with the solvent than just an implicit model. We find stabilising π-type interactions with the conjugated DMA solvent (Fig. 1c) and calculate an improved 85 : 15 dr, in closer agreement with the experimental dr (72 : 28 dr). Similarly, the dr can be improved by scaling the solvent cavity, which in turn is constructed from the van der Waals radii (Fig. 1d). With a larger cavity, there is a greater separation between the large molecular dipole and the dielectric medium which leads to a reduction in coulombic interaction. This is larger for the minor TS than the major TS due to the larger dipole moment ( $\mu = 29.54$  and 19.84 D, respectively).

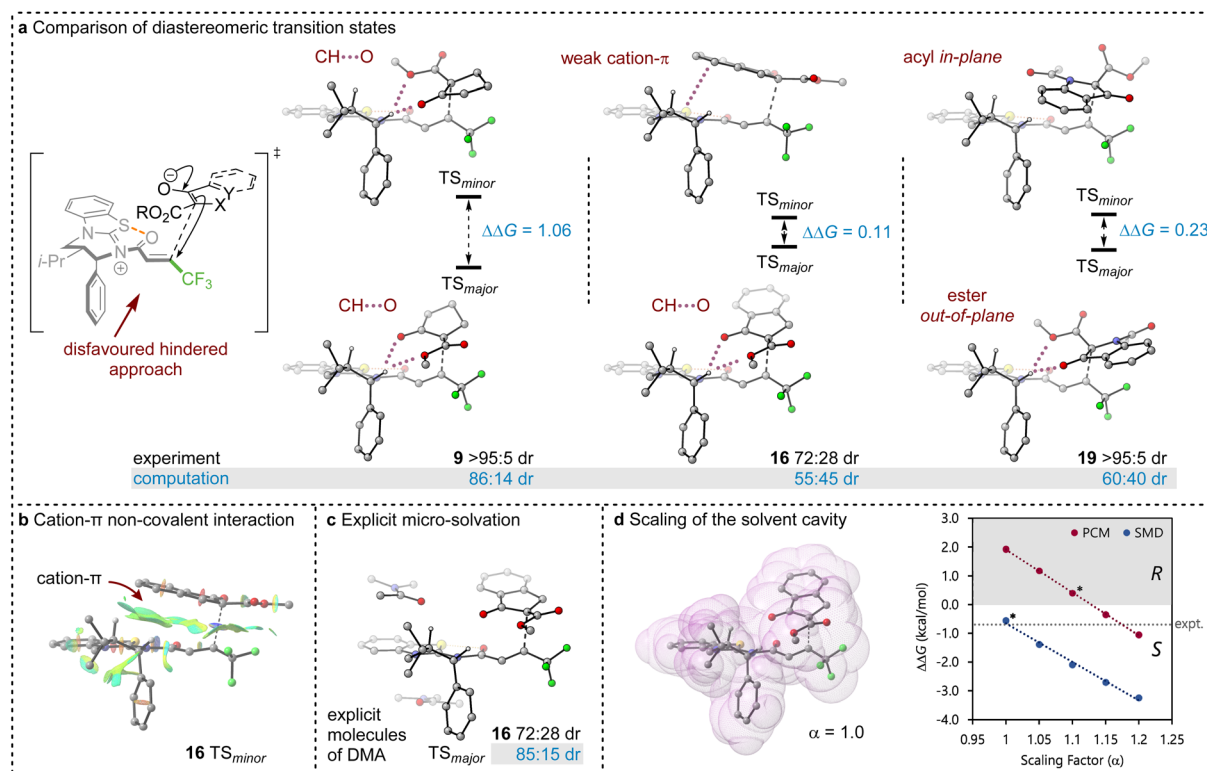


Fig. 1 (a) DFT analysis of the most stable major and minor diastereomeric transition states. Important interactions are highlighted, with dual CH···O interactions present in all major TS. M06-2X<sub>SMD</sub>/def2-TZVP//M06-2X<sub>SMD</sub>/def2-SVP free energies ( $\Delta G_{298}$ ) are shown in kcal mol<sup>-1</sup> and selected hydrogen atoms have been removed for clarity. (b) Non-covalent interaction of key cation–π stabilisation of minor diastereomeric TS of **16**. (c) Explicit micro-solvation with π-type interaction with conjugated DMA solvent (with PCM solvation model). (d) Solvent cavity as a sum of van der Waals radii and graph of the selectivity ( $\Delta \Delta G_{298}$ ) as a function of the scaling parameter. Asterisks indicate the default value of  $\alpha$  for each solvent model.



Both approaches introduce a greater separation between the highly charged or dipolar regions of the TS and the dielectric medium and reduce the relative overstabilisation of the minor diastereomeric TS. Unfortunately, both approaches are undesirable from a methodological point of view. Explicit micro-solvation requires vast exploration of solvation sites and conformers, ultimately calling for extensive molecular dynamics simulations to sample the relevant minima in an ensemble, and artificially tweaking parameters of a solvent model may reduce its predictive power and general applicability.

Pleasingly, the Solvation Model based on Density (SMD) correctly reproduces the major diastereoisomer without scaling the solvent cavity or introducing micro-solvation. This model includes parameterisation to account for some of the dispersive interactions between the solute and solvent, mimicking the increased accuracy brought about by micro-solvation, whilst using a smaller solvent cavity than PCM. This model appears to help in stabilising the major diastereoisomer, presumably due to the parameterised dispersive interactions in its construction even with a reduced solvent cavity compared to PCM.

### 3 Conclusions

In conclusion, the enantioselective conjugate addition of a range of carbo- and heterocyclic  $\alpha$ -substituted  $\beta$ -ketoesters to  $\alpha,\beta$ -unsaturated aryl esters using the isothiourea HyperBTM 1 as a Lewis base catalyst has been demonstrated. Divergent diastereoselectivity is observed through judicious choice of pronucleophile, with either cyclopentanone-derived or indanone-derived substituted  $\beta$ -ketoesters generating divergent stereo-defined products with high stereoselectivity ( $>95:5$  dr, up to  $99:1$  er). The scope and limitations of these processes are demonstrated, alongside application on gram scale. Competitive isomerisation alongside conjugate addition is observed with (*Z*)-enoates. The origin of the divergent stereoselectivity has been studied using DFT and can be attributed to a variety of weak non-covalent interactions between the  $\alpha,\beta$ -unsaturated acyl isothiouronium intermediate and the incoming nucleophile. These weak attractive interactions modulate the steric repulsion from the stereodirecting C(2)-phenyl substituent within the catalyst–substrate  $\alpha,\beta$ -unsaturated acyl isothiouronium intermediate and need to be accounted for by the computational methodology. Because the key TSs are highly polar, an adequate treatment of solvation effects in the model is instrumental. Building upon this work and the insights gained from DFT analysis, further applications of related reaction processes are currently under investigation in this laboratory.<sup>53</sup>

### Data availability

The research data supporting this publication can be accessed at: <https://doi.org/10.17630/013114f4-2dbc-49ae-b64a-97d34f222a34>.

### Author contributions

ADS and GRB conceived the project; DY, ZD and GRB carried out all experimental studies in consultation with TK and KK.

ADS, DY, KK, ASG and GRB wrote the manuscript. DBC and APM carried out single crystal X-ray analysis. ASG carried out all computation in consultation with MB. All authors agreed on the finalised version of the manuscript.

### Conflicts of interest

There are no conflicts to declare.

### Acknowledgements

The research leading to these results has received funding from the CSC (DY), the EPSRC (TK, KK, EP/T023643/1) and the EASI-CAT centre for Doctoral Training (ASG). ADS thanks the EPSRC Programme Grant “Boron: Beyond the Reagent” (EP/W007517) for support. MB thanks EaStCHEM and the School of Chemistry for support. Computations were performed on a local HPC cluster maintained by Dr H. Frücht. GRB is grateful to Florida Gulf Coast University (FGCU) for a sabbatical award.

### References

- Y. Liu, S. J. Han, W. B. Liu and B. M. Stoltz, Catalytic Enantioselective Construction of Quaternary Stereocenters: Assembly of Key Building Blocks for the Synthesis of Biologically Active Molecules, *Acc. Chem. Res.*, 2015, **48**(3), 740–751.
- T. Ling and F. Rivas, All-Carbon Quaternary Centers in Natural Products and Medicinal Chemistry: Recent Advances, *Tetrahedron*, 2016, **72**(43), 6729–6777.
- Y. Hamashima, D. Hotta, N. Umebayashi, Y. Tsuchiya, T. Suzuki and M. Sodeoka, Catalytic Enantioselective Michael Reaction of 1,3-Dicarbonyl Compounds *via* Formation of Chiral Palladium Enolate, *Adv. Synth. Catal.*, 2005, **347**(11–13), 1576–1586.
- J. Yang, W. Li, Z. Jin, X. Liang and J. Ye, Enantioselective Michael Reaction of  $\alpha$ -Alkyl- $\beta$ -keto Esters and Enones under Multifunctional Catalysis, *Org. Lett.*, 2010, **12**(22), 5218–5221.
- K. Murai, S. Fukushima, A. Nakamura, M. Shimura and H. Fujioka, C3-Symmetric chiral trisimidazoline: the role of a third imidazoline and its application to the nitro Michael reaction and the  $\alpha$ -amination of  $\beta$ -ketoesters, *Tetrahedron*, 2011, **67**(26), 4862–4868.
- S. Riko, J. Svete, B. Tefane, A. Perdih and U. Groelj, 1,3-Diamine-Derived Bifunctional Organocatalyst Prepared from Camphor, *Adv. Synth. Catal.*, 2016, **358**(23), 3786–3796.
- G. Chen, G. Liang, Y. Wang, P. Deng and H. Zhou, A homodinuclear cobalt complex for the catalytic asymmetric Michael reaction of  $\beta$ -ketoesters to nitroolefins, *Org. Biomol. Chem.*, 2018, **16**(20), 3841–3850.
- L.-K. Wang, J.-J. Zhou, Y.-B. Lan, S.-Y. Ding, W. Yu and W. Wang, Divergent Synthesis of Chiral Covalent Organic Frameworks, *Angew. Chem., Int. Ed.*, 2019, **58**(28), 9443.
- C. Kabes, R. Lucas, J. Gunn and J. Gladysz, Chiral Cobalt(III) Tris(1,2-diamine) Catalysts That Incorporate Nitrogenous Base Containing Anions for the Bifunctional Activation of



- Nucleophiles and Electrophiles in Enantioselective Addition Reactions, *ACS Catal.*, 2021, **11**(13), 7762–7771.
- 10 F. Wu, H. Li, R. Hong and L. Deng, Construction of Quaternary Stereocenters by Efficient and Practical Conjugate Additions to  $\alpha,\beta$ -Unsaturated Ketones with a Chiral Organic Catalyst, *Angew. Chem., Int. Ed.*, 2005, **45**(6), 947–950.
- 11 H. J. Loui and C. Schneider, Cooperative Palladium/Brønsted Acid Catalysis toward the Highly Enantioselective Allenylation of  $\beta$ -Keto Esters, *Org. Lett.*, 2022, **24**(7), 1496–1501.
- 12 Y. Hamashima, D. Hotta and M. Sodeoka, Direct Generation of Nucleophilic Chiral Palladium Enolate from 1,3-Dicaronyl Compounds: Catalytic Enantioselective Michael Reaction with Enones, *J. Am. Chem. Soc.*, 2002, **124**(38), 11240–11241.
- 13 J. Liu, Z. Han, X. Wang, F. Meng, Z. Wang and K. Ding, Palladium-Catalyzed Asymmetric Construction of Vicinal Tertiary and All-Carbon Quaternary Stereocenters by Allylation of  $\beta$ -Ketocarbonyls with Morita–Baylis–Hillman Adducts, *Angew. Chem., Int. Ed.*, 2017, **56**(18), 5050–5054.
- 14 For general reviews of isothiourea reactivity see: (a) J. E. Taylor, S. D. Bull and J. M. Williams, Amidines, isothioureas, and guanidines as nucleophilic catalysts, *Chem. Soc. Rev.*, 2012, **41**(6), 2109–2121; (b) V. B. Birman, Amidine-Based catalysts: Design, Development and Applications, *Aldrichimica Acta*, 2016, **49**(2), 23–33; (c) J. Merad, J.-M. Pons, O. Chuzel and C. Bressy, Enantioselective Catalysis by Chiral Isothioureas, *Eur. J. Org. Chem.*, 2016, **2016**(34), 5589–5610; (d) A. Biswas, H. Mondal and M. S. Maji, Synthesis of Heterocycles by isothiourea organocatalysis, *J. Heterocycl. Chem.*, 2020, **57**(11), 2828–3844.
- 15 For reviews of this area see: (a) S. Vellalath and D. Romo, Asymmetric Organocatalysis: The Emerging Utility of  $\alpha,\beta$ -Unsaturated Acylammonium Salts, *Angew. Chem., Int. Ed.*, 2016, **55**(45), 13934–13943; (b) J. Bitai, M. T. Westwood and A. D. Smith,  $\beta$ -Unsaturated acyl ammonium species as reactive intermediates in organocatalysis: an update, *Org. Biomol. Chem.*, 2021, **19**(11), 2366–2384.
- 16 C. McLaughlin and A. D. Smith, Generation and Reactivity of C(1)-Ammonium Enolates by Using Isothiourea Catalysis, *Chem.–Eur. J.*, 2021, **27**(5), 1533–1555.
- 17 E. R. T. Robinson, C. Fallan, C. Simal, A. M. Z. Slawin and A. D. Smith, Anhydrides as  $\alpha,\beta$ -unsaturated acyl ammonium precursors: isothiourea-promoted catalytic asymmetric annulation processes, *Chem. Sci.*, 2013, **4**(5), 2193–2200.
- 18 G. Liu, M. E. Shirley, K. N. Van, R. L. McFarlin and D. Romo, Rapid assembly of complex cyclopentanes employing chiral,  $\alpha,\beta$ -unsaturated acylammonium intermediates, *Nat. Chem.*, 2013, **5**(12), 1049–1057.
- 19 A. Matviitsuk, M. D. Greenhalgh, D. J. Barrios Antuñez, A. M. Z. Slawin and A. D. Smith, Aryloxide-Facilitated Catalyst Turnover in Enantioselective  $\alpha,\beta$ -Unsaturated Acyl Ammonium Catalysis, *Angew. Chem., Int. Ed.*, 2017, **56**(40), 12282–12287.
- 20 Y. Fukata, K. Asano and S. Matsubara, Facile Net Cycloaddition Approach to Optically Active 1,5-Benzothiazepines, *J. Am. Chem. Soc.*, 2015, **137**(16), 5320–5323.
- 21 J.-H. Jin, X.-Y. Li, X. Luo and W.-P. Deng, Enantioselective synthesis of indolo[2,3-*b*]-dihydrothiopyranones *via* [3+3] cycloaddition of chiral  $\alpha,\beta$ -unsaturated acylammonium salts, *Tetrahedron*, 2018, **74**(47), 6804–6808.
- 22 T. Kurihara, M. Kojima, T. Yoshino and S. Matsunaga, Achiral Cp<sup>\*</sup>Rh(III)/Chiral Lewis Base Cooperative Catalysis for Enantioselective Cyclisation *via* C–H Activation, *J. Am. Chem. Soc.*, 2022, **144**(16), 7058–7065.
- 23 E. R. T. Robinson, D. M. Walden, C. Fallan, M. D. Greenhalgh, P. H.-Y. Cheong and A. D. Smith, Non-bonding 1,5-S···O interactions govern chemo- and enantioselectivity in isothiourea-catalyzed annulations of benzazoles, *Chem. Sci.*, 2016, **7**(12), 6919–6927.
- 24 W. C. Hartley, T. J. C. O’Riordan and A. D. Smith, Aryloxide-Promoted Catalyst Turnover in Lewis Base Organocatalysis, *Synthesis*, 2017, **49**(15), 3303–3310.
- 25 H. Liu, A. M. Z. Slawin and A. D. Smith, Isothiourea-Catalyzed Enantioselective Synthesis of Tetrahydro- $\alpha$ -carbolinones, *Org. Lett.*, 2020, **22**(4), 1301–1305.
- 26 J. Wu, C. M. Young, A. A. Watts, A. M. Z. Slawin, G. R. Boyce, M. Bühl and A. D. Smith, Isothiourea-Catalyzed Enantioselective Michael Addition of Malonates to  $\alpha,\beta$ -Unsaturated Aryl Esters, *Org. Lett.*, 2022, **24**(22), 4040–4045.
- 27 J. E. Lapetaje, C. M. Young, C. Shu and A. D. Smith, Isothiourea-catalyzed formal enantioselective conjugate addition of benzophenone imines to  $\beta$ -fluorinated  $\alpha,\beta$ -unsaturated esters, *Chem. Commun.*, 2022, **58**(49), 6886–6889.
- 28 (a) J. Bitai, A. J. Nimmo, A. M. Z. Slawin and A. D. Smith, Cooperative Palladium/Isothiourea Catalyzed Enantioselective Formal (3+2) Cycloaddition of Vinylcyclopropanes and  $\alpha,\beta$ -Unsaturated Esters, *Angew. Chem., Int. Ed.*, 2022, **61**(25), e202202621; (b) J. Bitai, A. M. Z. Slawin, D. B. Cordes and A. D. Smith, Exploring the Scope of Tandem Palladium and Isothiourea Relay Catalysis for the Synthesis of  $\alpha$ -Amino Acid Derivatives, *Molecules*, 2020, **25**(10), 2463.
- 29 M. D. Greenhalgh, S. Qu, A. M. Z. Slawin and A. D. Smith, Multiple roles of aryloxide leaving groups in enantioselective annulations employing  $\alpha,\beta$ -unsaturated acyl ammonium catalysis, *Chem. Sci.*, 2018, **9**(21), 4909–4918.
- 30 C. Wang, S.-J. Li, Q.-C. Zhang, D. Wei and L. Ding, Insights into isothiourea-catalyzed asymmetric [3 + 3] annulation of  $\alpha,\beta$ -unsaturated aryl esters with 2-acylbenzazoles: mechanism, origin of selectivity and switchable chemoselectivity, *Catal. Sci. Technol.*, 2020, **10**(11), 3664–3669.
- 31 CCDC 2298980 contains the supplementary crystallographic data for (1*S*,2*S*’)-9.
- 32 CCDC 2298981 contains the supplementary crystallographic data for (2*S*,2*S*’)-16.



- 33 CCDC 2298982 contains the supplementary crystallographic data for (2S,2'S)-20.
- 34 L. C. Morrill, J. J. Douglas, T. Lebl, A. M. Z. Slawin, D. J. Fox and A. D. Smith, Isothiourea-mediated asymmetric Michael-lactonisation of trifluoromethylenones: a synthetic and mechanistic study, *Chem. Sci.*, 2013, **4**(11), 4146–4155.
- 35 C. Shu, H. Liu, A. M. Z. Slawin, C. Carpenter-Warren and A. D. Smith, Isothiourea-catalysed enantioselective Michael addition of N-heterocyclic pronucleophiles to  $\alpha,\beta$ -unsaturated aryl esters, *Chem. Sci.*, 2020, **11**(1), 241–247.
- 36 For an early theoretical investigation of chalcogen-bonding, see: C. Bleiholder, R. Gleiter, D. B. Werz and H. Köppel, Theoretical Investigations on Heteronuclear Chalcogen-Chalcogen Interactions: On the Nature of Weak Bonds between Chalcogen Centers, *Inorg. Chem.*, 2007, **46**(6), 2249–2260.
- 37 For a recent review on chalcogen-bonding, see: R. Gleiter, G. Haberhauer, D. B. Werz, F. Rominger and C. Bleiholder, From Noncovalent Chalcogen–Chalcogen Interactions to Supramolecular Aggregates: Experiments and Calculations, *Chem. Rev.*, 2018, **118**(4), 2010–2041.
- 38 For a recent perspective on chalcogen-bonding see: S. Kolb, G. A. Oliver and D. B. Werz, Chemistry Evolves, Terms Evolve, but Phenomena Do Not Evolve: From Chalcogen–Chalcogen Interactions to Calcogen Bonding, *Angew. Chem., Int. Ed.*, 2020, **59**(50), 22306–22310.
- 39 For a discussion on the origin of chalcogen-bonding interactions, see: D. J. Pascoe, K. B. Ling and S. L. Cockcroft, The Origin of Chalcogen-Bonding Interactions, *J. Am. Chem. Soc.*, 2017, **139**(42), 15160–15167.
- 40 For selected examples of chalcogen bonding catalysis see (a) S. Benz, J. López-Andarias, J. Mareda, N. Sakai and S. Matile, Catalysis with Chalcogen Bonds, *Angew. Chem., Int. Ed.*, 2017, **56**(3), 812–815; (b) P. Wonner, L. Vogel, M. Düser, L. Gomes, F. Kniep, B. Mallick, D. B. Werz and S. M. Huber, Carbon-Halogen Bond Activation by Selenium-Based Chalcogen Bonding, *Angew. Chem., Int. Ed.*, 2017, **56**(39), 12009–12012; (c) P. Wonner, L. Vogel, F. Kniep and S. M. Huber, Catalytic Carbon-Chlorine Bond Activation by Selenium-Based Chalcogen Bond Donors, *Chem.-Eur. J.*, 2017, **23**(67), 16972–16975; (d) P. Wonner, A. Dreger, E. Engelage and S. M. Huber, Chalcogen Bonding Catalysis of a Nitro-Michael Reaction, *Angew. Chem., Int. Ed.*, 2019, **58**(47), 16923–16927; (e) W. Wang, H. Zhu, S. Liu, Z. Zhao, L. Zhang, J. Hao and Y. Wang, Chalcogen–Chalcogen Bonding Catalysis Enables Assembly of Discrete Molecules, *J. Am. Chem. Soc.*, 2019, **141**(23), 9175–9179; (f) W. Wang, H. Zhu, L. Feng, Q. Yu, J. Hao, R. Zhu and Y. Wang, Dual Chalcogen–Chalcogen Bonding Catalysis, *J. Am. Chem. Soc.*, 2020, **142**(6), 3117–3124.
- 41 For discussions of S···O interactions in isothiourea catalysis: (a) V. B. Birman, X. Li and Z. Han, Nonaromatic Amidine Derivatives as Acylation Catalysts, *Org. Lett.*, 2007, **9**(1), 37–40; (b) P. Liu, X. Yang, V. B. Birman and K. N. Houk, Origin of Enantioselectivity in Benzotetramisole-Catalyzed Dynamic Kinetic Resolution of Azlactones, *Org. Lett.*, 2012, **14**(13), 3288–3291; (c) M. E. Abbasov, B. M. Hudson, D. J. Tantillo and D. Romo, Acylammonium Salts as Dienophiles in Diels-Alder/Lactonization Organocascades, *J. Am. Chem. Soc.*, 2014, **136**(12), 4492–4495; (d) M. D. Greenhalgh, S. M. Smith, D. M. Walden, J. E. Taylor, Z. Brice, E. R. T. Robinson, C. Fallan, D. B. Cordes, A. M. Z. Slawin, H. C. Richardson, M. A. Grove, P. H.-Y. Cheong and A. D. Smith, A C=O···Isothiouronium Interaction Dictates Enantiodiscrimination in Acylatice Kinetic Resolutions of Tertiary Heterocycl Alcohols, *Angew. Chem., Int. Ed.*, 2018, **57**(12), 3200–3206; (e) C. M. Young, A. Elmi, D. J. Pascoe, R. K. Morris, C. McLaughlin, A. M. Woods, A. B. Frost, A. de la Houpliere, K. B. Ling, T. K. Smith, A. M. Z. Slawin, P. H. Willoughby, S. L. Cockcroft and A. D. Smith, The Importance of 1,5-Oxygen···Chalcogen Interactions in Enantioselective Isochalcogenourea Catalysis, *Angew. Chem., Int. Ed.*, 2020, **59**(9), 3705–3710.
- 42 For use of S···O interaction in asymmetric synthesis, see: Y. Nagao, S. Miyamoto, M. Miyamoto, H. Takeshige, K. Hayashi, S. Sano, M. Shiro, K. Yamaguchi and Y. Sei, Highly Stereoselective Asymmetric Pummerer Reactions That Incorporate Intermolecular and Intramolecular Nonbonded S···O Interactions, *J. Am. Chem. Soc.*, 2006, **128**(30), 9722–9729.
- 43 For examples of S···O interactions in medicinal chemistry, see: B. R. Beno, K.-S. Yeung, M. D. Bartberger, L. D. Pennington and N. A. Meanwell, *J. Med. Chem., A Survey of the Role of Noncovalent Sulfur Interactions in Drug Design*, 2015, **58**(11), 4383–4438.
- 44 Y. Zhao and D. G. Truhlar, The M06 suite of density functionals for main group thermochemistry, thermochemical kinetics, noncovalent interactions, excited states, and transition elements: Two new functionals and systematic testing of four M06-class functionals and 12 other functionals, *Theor. Chem. Acc.*, 2008, **120**(1), 215–241.
- 45 A. Schäfer, H. Horn and R. Ahlrichs, Fully optimized contracted Gaussian basis sets for atoms Li to Kr, *J. Chem. Phys.*, 1992, **97**(4), 2571–2577.
- 46 A. Schäfer, C. Huber and R. Ahlrichs, Fully optimized contracted Gaussian basis sets of triple zeta valence quality for atoms Li to Kr, *J. Chem. Phys.*, 1994, **100**(8), 5829–5835.
- 47 F. Weigend and R. Ahlrichs, Balanced basis sets of split valence, triple zeta valence and quadruple zeta valence quality for H to Rn: design and assessment of accuracy, *Phys. Chem. Chem. Phys.*, 2005, **7**(18), 3297–3305.
- 48 F. Weigend, Accurate Coulomb-fitting basis sets for H to Rn, *Phys. Chem. Chem. Phys.*, 2006, **8**(9), 1057–1065.
- 49 A. V. Marenich, C. J. Cramer and D. G. Truhlar, Universal solvation model based on solute electron density and on a continuum model of the solvent defined by the bulk dielectric constant and atomic surface tensions, *J. Phys. Chem. B*, 2009, **113**(18), 6378–6396.
- 50 M. J. Frisch, G. W. Trucks, H. B. Schlegel, G. E. Scuseria, M. A. Robb, J. R. Cheeseman, G. Scalmani, V. Barone, G. A. Petersson, H. Nakatsuji, X. Li, M. Caricato, A. V. Marenich, J. Bloino, B. G. Janesko, R. Gomperts, B. Mennucci, H. P. Hratchian, J. V. Ortiz, A. F. Izmaylov,



J. L. Sonnenberg, D. Williams-Young, F. Ding, F. Lipparini, F. Egidi, J. Goings, B. Peng, A. Petrone, T. Henderson, D. Ranasinghe, V. G. Zakrzewski, J. Gao, N. Rega, G. Zheng, W. Liang, M. Hada, M. Ehara, K. Toyota, R. Fukuda, J. Hasegawa, M. Ishida, T. Nakajima, Y. Honda, O. Kitao, H. Nakai, T. Vreven, K. Throssell, J. A. Montgomery, Jr, J. E. Peralta, F. Ogliaro, M. J. Bearpark, J. J. Heyd, E. N. Brothers, K. N. Kudin, V. N. Staroverov, T. A. Keith, R. Kobayashi, J. Normand, K. Raghavachari, A. P. Rendell, J. C. Burant, S. S. Iyengar, J. Tomasi, M. Cossi, J. M. Millam, M. Klene, C. Adamo, R. Cammi, J. W. Ochterski, R. L. Martin, K. Morokuma, O. Farkas, J. B. Foresman and D. J. Fox, *Gaussian 16, Revision C.01*, Gaussian Inc., Wallingford CT, 2019.

- 51 B. Mennucci and J. Tomasi, Continuum solvation models: a new approach to the problem of solute's charge distribution and cavity boundaries, *J. Chem. Phys.*, 1997, **106**(12), 5151–5158.
- 52 J. Tomasi, B. Mennucci and E. Cancès, The IEF version of the PCM solvation method: an overview of a new method addressed to study molecular solutes at the QM *ab initio* level, *J. Mol. Struct.*, 1999, **464**(1), 211–226.
- 53 *Understanding Divergent Substrate Stereoselectivity in the Enantioselective Isothiourea-Catalysed Conjugate Addition of Cyclic  $\alpha$ -substituted  $\beta$ -ketoesters to  $\alpha,\beta$ -unsaturated Aryl Esters*, University of St Andrews Research Portal, PURE ID: 29438761.

